



TECHNISCHE
UNIVERSITÄT
WIEN

FWF Österreichischer
Wissenschaftsfonds

$\int dk \Pi$

Doktoratskolleg
Particles and Interactions

Hard probes during the initial stages in heavy-ion collisions

Based on 2303.12520, 2303.12595, 2312.00447 and 2312.11252
(in collaboration with K. Boguslavski, A. Kurkela, T. Lappi, J. Peuron)

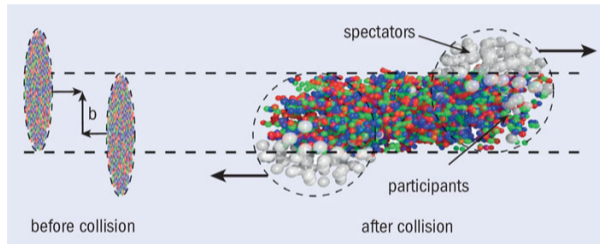
Florian Lindenbauer

TU Wien

26.06.2024, QCD Master Class, Saint-Jacut-de-la-Mer

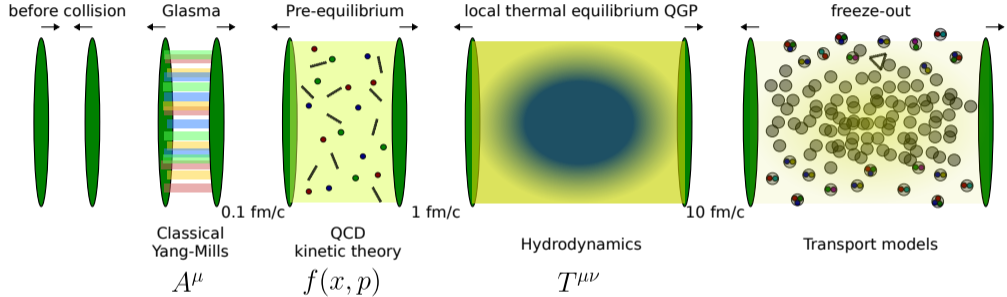
- 1 Introduction
- 2 Jet quenching parameter
- 3 Heavy quark diffusion coefficient
- 4 Limiting attractors
- 5 Conclusion

- Study high-temperature properties of the strong interaction
- Collision of atomic nuclei at LHC or RHIC
- Creates high-temperature QCD matter = Quark-Gluon plasma (QGP)



[Alberica Toia 2013, CERN COURIER]

Time-evolution of the QGP in heavy-ion collisions

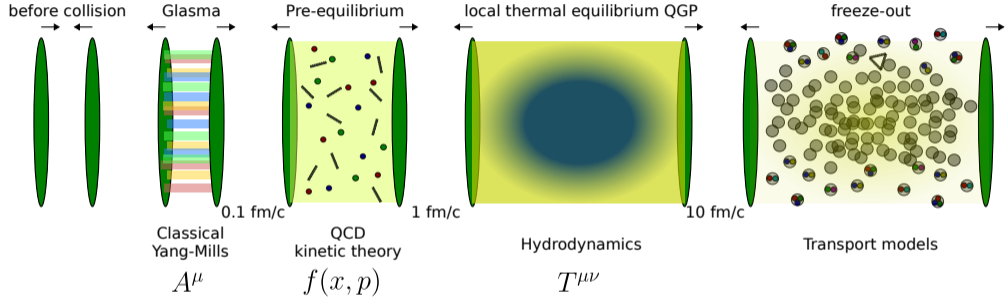


Interested in pre-equilibrium stages (“Initial stages”)

→ **QCD out of equilibrium**

[Rev.Mod.Phys. 93 (2021) [Berges, Heller, Mazeliauskas, Venugopalan]]

Time-evolution of the QGP in heavy-ion collisions

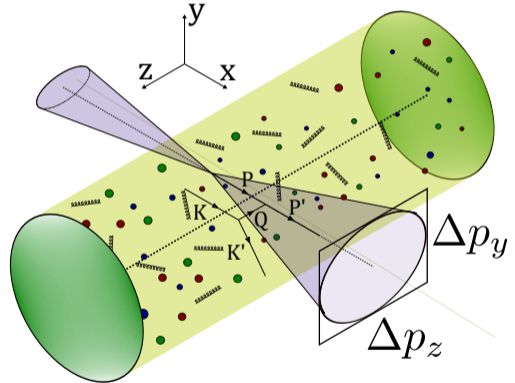


Interested in pre-equilibrium stages ("Initial stages")
 → **QCD out of equilibrium** (sign problem in lattice QCD)

[Rev.Mod.Phys. 93 (2021) [Berges, Heller, Mazeliauskas, Venugopalan]]

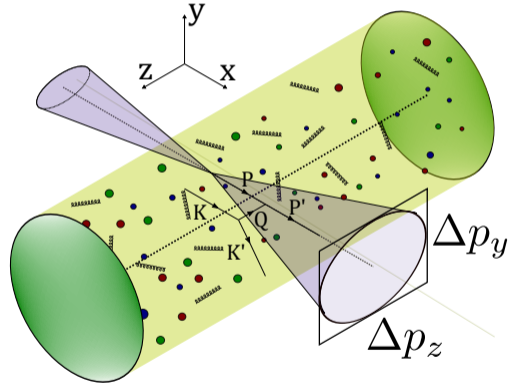
How can we study the initial stages?

- To study initial stages
→ very **energetic** or **heavy** probes
(must be created early)
- Here depicted: **jets**



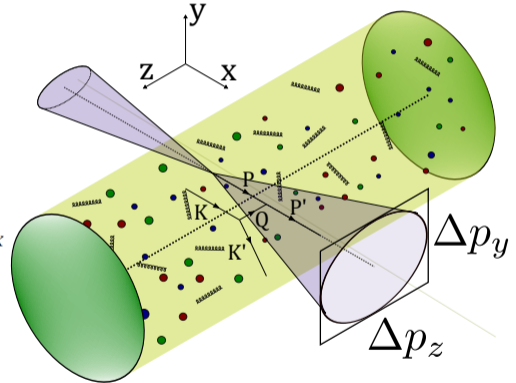
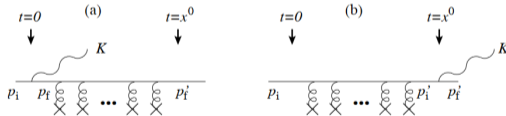
How can we study the initial stages?

- To study initial stages
→ very **energetic** or **heavy** probes
(must be created early)
- Here depicted: **jets**
 - **Highly energetic partons**
created in initial collision
 - Splits into many particles
→ then measured in the detectors
 - Imprints of **medium interactions**



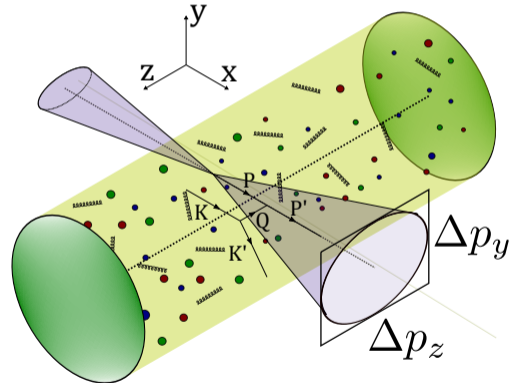
Jet energy loss through medium-induced radiation

- Very many works on energy loss of energetic parton
- Difficulties:**
Including the LPM effect



Jet energy loss through medium-induced radiation

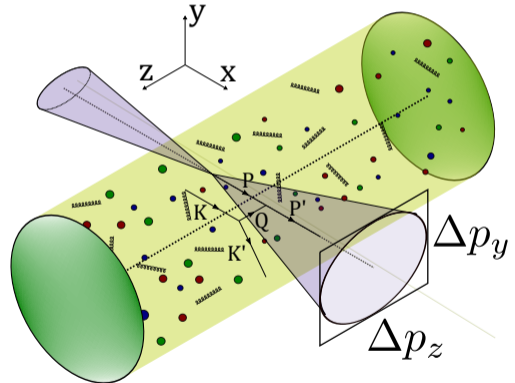
- Very many works on energy loss of energetic parton
- **Difficulties:**
Including the LPM effect
- **Harmonic approximation:**
Depend on single medium parameter \hat{q}
“Jet quenching parameter”



Jet energy loss through medium-induced radiation

- Very many works on energy loss of energetic parton
- **Difficulties:**
Including the LPM effect
- **Harmonic approximation:**
Depend on single medium parameter \hat{q}
“**Jet quenching parameter**”
- Quantifies **momentum broadening**

$$\hat{q} = \frac{d\langle p_{\perp}^2 \rangle}{dL} = \frac{d\langle p_{\perp}^2 \rangle}{dt} = \int d^2 q_{\perp} q_{\perp}^2 \frac{d\Gamma^{\text{el}}}{d^2 q_{\perp}}$$





Physics Letters B

Volume 803, 10 April 2020, 135318



Jet quenching as a probe of the initial stages in heavy-ion collisions ☆

[Carlota Andres](#)^a  , [Néstor Armesto](#)^b , [Harri Niemi](#)^{c,d} , [Risto Paatelainen](#)^{e,d} ,
[Carlos A. Salgado](#)^b 

ABSTRACT

Jet quenching provides a very flexible variety of observables which are sensitive to different energy- and time-scales of the strongly interacting matter created in heavy-ion collisions. Exploiting this versatility would make jet quenching an excellent chronometer of the yoctosecond structure of the evolution process. Here we show, for the first time, that a combination of jet quenching observables is sensitive to the initial stages of heavy-ion collisions, when the approach to local thermal equilibrium is expected to happen. Specifically, we find that in order to reproduce at the same time the inclusive particle production suppression, R_{AA} , and the high- p_T azimuthal asymmetries, v_2 , energy loss must be strongly suppressed for the first ~ 0.6 fm. This exploratory analysis shows the potential of jet observables, possibly more sophisticated than the ones studied here, to constrain the dynamics of the initial stages of the evolution.

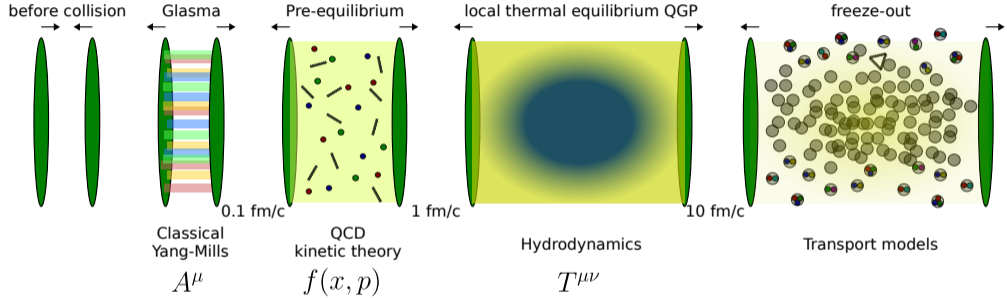
© 2020 The Author(s). Published by Elsevier B.V. This is an open access article under the CC BY license (<http://creativecommons.org/licenses/by/4.0/>). Funded by SCOAP³.

A B S T R A C T

Jet quenching provides a very flexible variety of observables which are sensitive to different energy- and time-scales of the strongly interacting matter created in heavy-ion collisions. Exploiting this versatility would make jet quenching an excellent chronometer of the yoctosecond structure of the evolution process. Here we show, for the first time, that a combination of jet quenching observables is sensitive to the initial stages of heavy-ion collisions, when the approach to local thermal equilibrium is expected to happen. Specifically, we find that in order to reproduce at the same time the inclusive particle production suppression, R_{AA} , and the high- p_T azimuthal asymmetries, v_2 , energy loss must be strongly suppressed for the first ~ 0.6 fm. This exploratory analysis shows the potential of jet observables, possibly more sophisticated than the ones studied here, to constrain the dynamics of the initial stages of the evolution.

© 2020 The Author(s). Published by Elsevier B.V. This is an open access article under the CC BY license (<http://creativecommons.org/licenses/by/4.0/>). Funded by SCOAP³.

Estimates of \hat{q}





Physics Letters B

Volume 834, 10 November 2022, 137464



Jet quenching in glasma

Margaret E. Carrington^{a,b}, Alina Czajka^c, Stanisław Mrówczyński^{c,d}  

\hat{q} in the glasma using τ expansion

In conclusion, our approach, which is presented in detail in [22], provides a reliable estimate of momentum broadening in glasma. Our calculation gives a value of \hat{q} that is several GeV^2/fm , which is much larger than equilibrium values, and produces accumulated transverse momentum broadening of the same order as the contribution from the equilibrium phase. Our results therefore indicate that the transient glasma phase plays an important role in the jet quenching. This conclusion is significant because it contradicts previous beliefs that the contribution to momentum broadening from the glasma phase can be safely neglected.



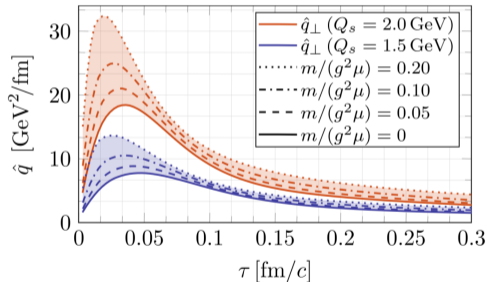
Physics Letters B
Volume 810, 10 November 2020, 135810



Jet momentum broadening in the pre-equilibrium Glasma

A. Ipp, D.I. Müller, D. Schuh

\hat{q} in the glasma using classical statistical simulations



PHYSICAL REVIEW D
covering particles, fields, gravitation, and cosmology

Highlights Recent Accepted Collections Authors Referees Search Press About

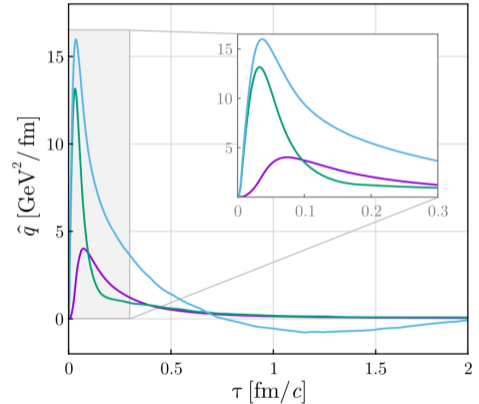
Open Access

Simulating jets and heavy quarks in the glasma using the colored particle-in-cell method

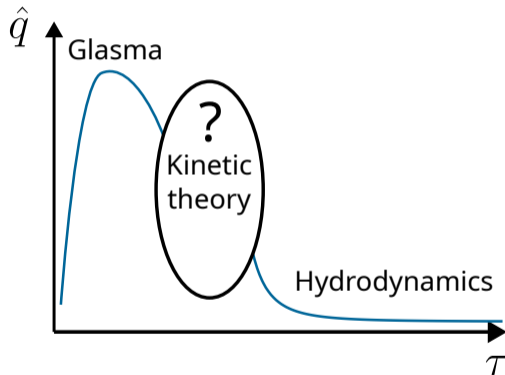
Dana Avramescu, Virgil Băran, Vincenzo Greco, Andreas Ipp, David Müller, and Marco Ruggieri
 Phys. Rev. D **107**, 114021 – Published 15 June 2023

Article References Citing Articles (2) PDF HTML Export Citation

\hat{q} in the glasma using classical statistical simulations



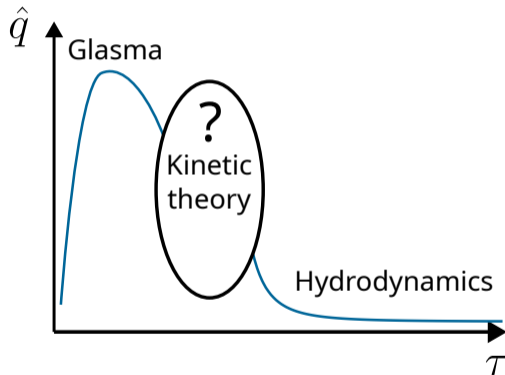
- **Mostly** considered in **equilibrium** or hydrodynamics

Schematic overview of \hat{q} evolution

¹[Phys.Lett.B 810 (2020) [Ipp, Müller, Schuh], Phys.Rev.C 105 (2022) [Carrington, Czajka, Mrowczynski], Phys.Rev.D 107 (2023)

[Avramescu, Baran, Greco, Ipp, Müller, Ruggieri]]

- **Mostly** considered in **equilibrium** or hydrodynamics
- Recently also considered in Glasma¹
- **Goal: \hat{q} during thermalization**
→ between Glasma and hydro
- **Question:**
Supports large Glasma values?

Schematic overview of \hat{q} evolution

¹[Phys.Lett.B 810 (2020) [Ipp, Müller, Schuh], Phys.Rev.C 105 (2022) [Carrington, Czajka, Mrowczynski], Phys.Rev.D 107 (2023)

[Avramescu, Baran, Greco, Ipp, Müller, Ruggieri]]

Effective kinetic theory description of the QGP

- Plasma without quarks

$$\mathcal{L} = -\frac{1}{4} F_{\mu\nu}^i F_i^{\mu\nu} + \bar{\psi}(i\not{D} - m)\psi$$

²[JHEP 01 (2003) [Arnold, Moore, Yaffe], Int.J.Mod.Phys.E 16 (2007) [Arnold]] 


Effective kinetic theory description of the QGP

- Plasma without quarks
- Gluons with **distribution function** $f(t, \mathbf{p})$
- Time evolution described by **Boltzmann equation** at leading-order²

$$(\partial_t + \mathbf{v} \cdot \nabla) f = \underbrace{\left| \begin{array}{c} \text{---} \\ \text{---} \\ \text{---} \\ \text{---} \\ \text{---} \\ \text{---} \end{array} \right|^2 + \left| \begin{array}{c} \text{---} \\ \text{---} \\ \text{---} \\ \text{---} \\ \text{---} \\ \text{---} \end{array} \right|^2}_{\text{Collision term}}$$

Collision term

- Azimuthal symmetry around beam axis \hat{z} ,
Bjorken expansion, homogeneous in transverse plane

²[JHEP 01 (2003) [Arnold, Moore, Yaffe], Int.J.Mod.Phys.E 16 (2007) [Arnold]] 

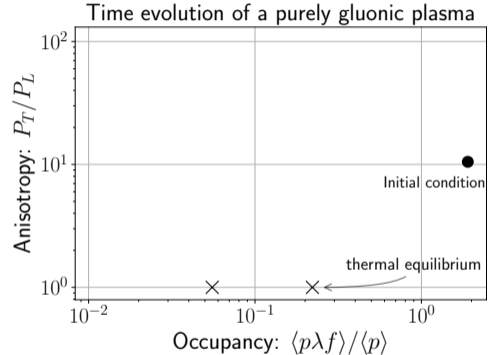
Bottom-up thermalization in heavy-ion collisions

- Initial condition³, with $\lambda = g^2 N_C$

$$f(p_\perp, p_z) = \frac{2A}{\lambda} \frac{\langle p_T \rangle}{\sqrt{p_\perp^2 + \xi^2 p_z^2}} \times \exp\left(\frac{-2}{3\langle p_T \rangle^2} (p_\perp^2 + \xi^2 p_z^2)\right)$$

$\xi \sim$ anisotropy, $\langle p_T \rangle = 1.8Q_s$,

$Q_s \sim$ saturation scale



³[Phys.Rev.Lett. 115 (2015) [Kurkela, Zhu]]

⁴[Phys.Lett.B 502 (2001) [Baier, Mueller, Schiff, Son]]

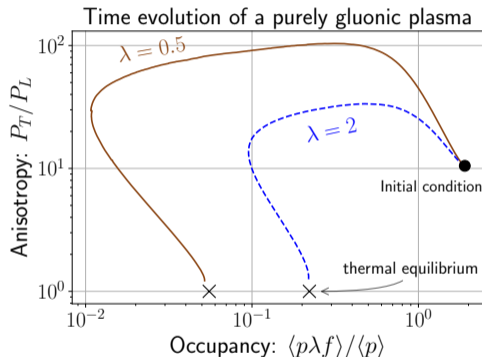
Bottom-up thermalization in heavy-ion collisions

- Initial condition³, with $\lambda = g^2 N_C$

$$f(p_\perp, p_z) = \frac{2A}{\lambda} \frac{\langle p_T \rangle}{\sqrt{p_\perp^2 + \xi^2 p_z^2}} \times \exp\left(\frac{-2}{3\langle p_T \rangle^2} (p_\perp^2 + \xi^2 p_z^2)\right)$$

$\xi \sim$ anisotropy, $\langle p_T \rangle = 1.8Q_s$,

$Q_s \sim$ saturation scale



³[Phys.Rev.Lett. 115 (2015) [Kurkela, Zhu]]

⁴[Phys.Lett.B 502 (2001) [Baier, Mueller, Schiff, Son]]

Bottom-up thermalization in heavy-ion collisions

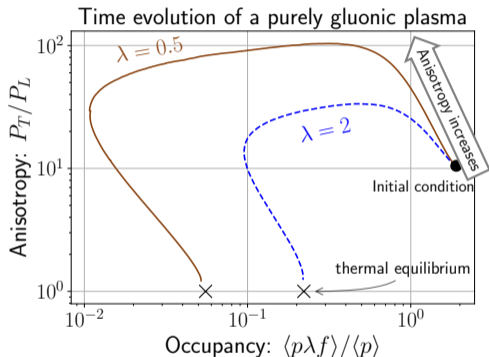
- Initial condition³, with $\lambda = g^2 N_C$

$$f(p_\perp, p_z) = \frac{2A}{\lambda} \frac{\langle p_T \rangle}{\sqrt{p_\perp^2 + \xi^2 p_z^2}} \times \exp\left(\frac{-2}{3\langle p_T \rangle^2} (p_\perp^2 + \xi^2 p_z^2)\right)$$

$\xi \sim$ anisotropy, $\langle p_T \rangle = 1.8Q_s$,

$Q_s \sim$ saturation scale

- Phase 1:** Anisotropy increases



³[Phys.Rev.Lett. 115 (2015) [Kurkela, Zhu]]

⁴[Phys.Lett.B 502 (2001) [Baier, Mueller, Schiff, Son]]

Bottom-up thermalization in heavy-ion collisions

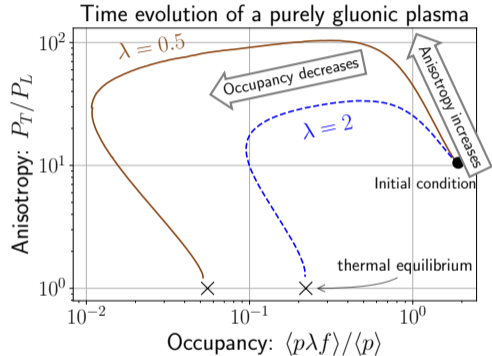
- Initial condition³, with $\lambda = g^2 N_C$

$$f(p_{\perp}, p_z) = \frac{2A}{\lambda} \frac{\langle p_T \rangle}{\sqrt{p_{\perp}^2 + \xi^2 p_z^2}} \times \exp\left(\frac{-2}{3\langle p_T \rangle^2} (p_{\perp}^2 + \xi^2 p_z^2)\right)$$

$\xi \sim$ anisotropy, $\langle p_T \rangle = 1.8Q_s$,

$Q_s \sim$ saturation scale

- Phase 1:** Anisotropy increases
- Phase 2:** Occupancy decreases



³[Phys.Rev.Lett. 115 (2015) [Kurkela, Zhu]]

⁴[Phys.Lett.B 502 (2001) [Baier, Mueller, Schiff, Son]]

Bottom-up thermalization in heavy-ion collisions

- Initial condition³, with $\lambda = g^2 N_C$

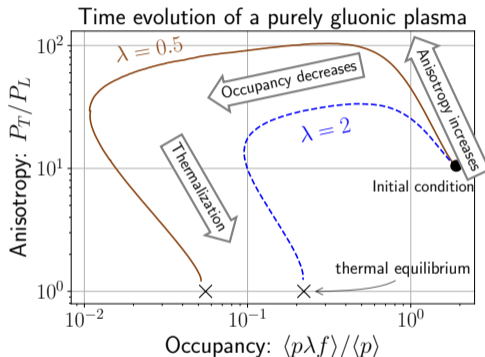
$$f(p_\perp, p_z) = \frac{2A}{\lambda} \frac{\langle p_T \rangle}{\sqrt{p_\perp^2 + \xi^2 p_z^2}} \times \exp\left(\frac{-2}{3\langle p_T \rangle^2} (p_\perp^2 + \xi^2 p_z^2)\right)$$

$\xi \sim$ anisotropy, $\langle p_T \rangle = 1.8Q_s$,

$Q_s \sim$ saturation scale

- Phase 1:** Anisotropy increases
- Phase 2:** Occupancy decreases
- Phase 3:** System thermalizes at

$$\text{time}^4 \tau_{\text{BMSS}} = \left(\frac{\lambda}{12\pi}\right)^{-13/5} / Q_s$$



³[Phys.Rev.Lett. 115 (2015) [Kurkela, Zhu]]

⁴[Phys.Lett.B 502 (2001) [Baier, Mueller, Schiff, Son]]

Bottom-up thermalization in heavy-ion collisions

- Initial condition³, with $\lambda = g^2 N_C$

$$f(p_\perp, p_z) = \frac{2A}{\lambda} \frac{\langle p_T \rangle}{\sqrt{p_\perp^2 + \xi^2 p_z^2}} \times \exp\left(\frac{-2}{3\langle p_T \rangle^2} (p_\perp^2 + \xi^2 p_z^2)\right)$$

$\xi \sim$ anisotropy, $\langle p_T \rangle = 1.8Q_s$,

$Q_s \sim$ saturation scale

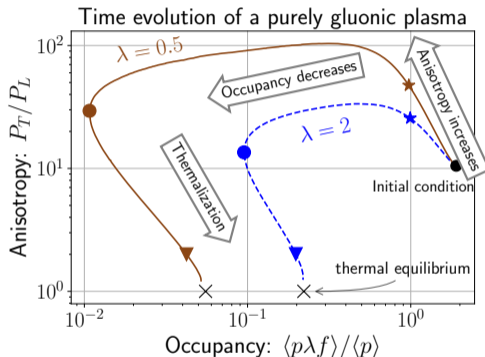
- Phase 1:** Anisotropy increases
- Phase 2:** Occupancy decreases
- Phase 3:** System thermalizes at

$$\text{time}^4 \tau_{\text{BMSS}} = \left(\frac{\lambda}{12\pi}\right)^{-13/5} / Q_s$$

Markers represent **different stages**

³[Phys.Rev.Lett. 115 (2015) [Kurkela, Zhu]]

⁴[Phys.Lett.B 502 (2001) [Baier, Mueller, Schiff, Son]]



Bottom-up thermalization in heavy-ion collisions

- Initial condition³, with $\lambda = g^2 N_C$

$$f(p_\perp, p_z) = \frac{2A}{\lambda} \frac{\langle p_T \rangle}{\sqrt{p_\perp^2 + \xi^2 p_z^2}} \times \exp\left(\frac{-2}{3\langle p_T \rangle^2} (p_\perp^2 + \xi^2 p_z^2)\right)$$

$\xi \sim$ anisotropy, $\langle p_T \rangle = 1.8Q_s$,

$Q_s \sim$ saturation scale

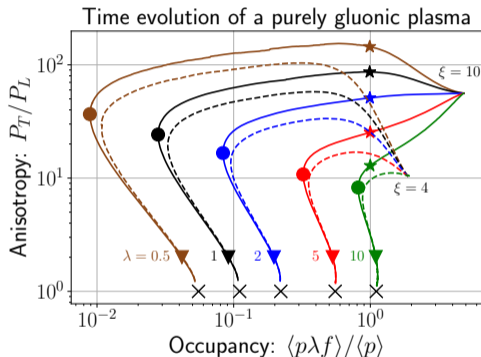
- Phase 1:** Anisotropy increases
- Phase 2:** Occupancy decreases
- Phase 3:** System thermalizes at

$$\text{time}^4 \tau_{\text{BMSS}} = \left(\frac{\lambda}{12\pi}\right)^{-13/5} / Q_s$$

Markers represent **different stages**

³[Phys.Rev.Lett. 115 (2015) [Kurkela, Zhu]]

⁴[Phys.Lett.B 502 (2001) [Baier, Mueller, Schiff, Son]]



Generalization of $\hat{q} \rightarrow \hat{q}^{ij}$ for anisotropic systems

- **Previously** (isotropic definition):

$$\hat{q} = \frac{d\langle p_{\perp}^2 \rangle}{dL} = \frac{d\langle p_{\perp}^2 \rangle}{dt} = \int d^2 q_{\perp} q_{\perp}^2 \frac{d\Gamma^{\text{el}}}{d^2 q_{\perp}}$$

with elastic scattering rate Γ^{el}

Generalization of $\hat{q} \rightarrow \hat{q}^{ij}$ for anisotropic systems

- **Previously** (isotropic definition):

$$\hat{q} = \frac{d\langle p_{\perp}^2 \rangle}{dL} = \frac{d\langle p_{\perp}^2 \rangle}{dt} = \int d^2 q_{\perp} q_{\perp}^2 \frac{d\Gamma^{\text{el}}}{d^2 q_{\perp}}$$

with elastic scattering rate Γ^{el}

- **To take into account anisotropies:**

Define matrix

$$\hat{q}^{ij} = \int d^2 q_{\perp} q_{\perp}^i q_{\perp}^j \frac{d\Gamma^{\text{el}}}{d^2 q_{\perp}}$$

Thus $\hat{q} = \hat{q}^{yy} + \hat{q}^{zz}$ (and $\hat{q}^{yz} = 0$)

- Provided we know $f(\mathbf{k})$:

Jet quenching parameter in kinetic theory

- Provided we know $f(\mathbf{k})$: Outgoing plasma particle

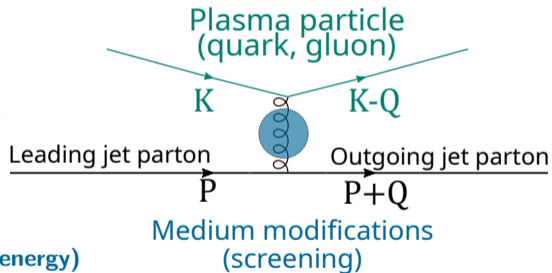
$$\hat{q}^{ij} = \int_{\substack{q_{\perp} < \Lambda \\ p \rightarrow \infty}} d\Gamma_{\text{PS}} q^i q^j |\mathcal{M}|^2 f(k) (1 + f(k'))$$

Incoming plasma particles
with momentum k

Matrix element
with medium corrections (self-energy)

appropriate phase-space measure

Matrix element



Making sense of the cutoff

- Cutoff Λ_{\perp} restricts transverse momentum transfer $q_{\perp} < \Lambda_{\perp}$
(needed in eikonal limit $p \rightarrow \infty$)

$$\hat{q} \sim \int d^2 q_{\perp} q_{\perp}^2 \underbrace{\frac{d\Gamma^{\text{el}}}{d^2 q_{\perp}}}_{1/q_{\perp}^4 \text{ for large } q_{\perp}} \sim \int \frac{dq_{\perp}}{q_{\perp}}$$

Making sense of the cutoff

- Cutoff Λ_{\perp} restricts transverse momentum transfer $q_{\perp} < \Lambda_{\perp}$
(needed in eikonal limit $p \rightarrow \infty$)
- Cutoff somehow grow with jet energy

[arXiv:2312.00447 [Boguslavski, Kurkela, Lappi, FL, Peuron]]

Making sense of the cutoff

- Cutoff Λ_{\perp} restricts transverse momentum transfer $q_{\perp} < \Lambda_{\perp}$
(needed in eikonal limit $p \rightarrow \infty$)
- Cutoff somehow grow with jet energy
- **kinematic cutoff** $\Lambda_{\perp}^{\text{kin}}(E, T) = \zeta^{\text{kin}} g(ET)^{1/2}$
obtained from comparing leading log behavior for large p and Λ_{\perp}

[arXiv:2312.00447 [Boguslavski, Kurkela, Lappi, FL, Peuron]]

Making sense of the cutoff

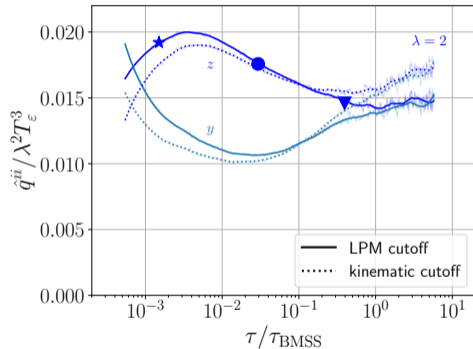
- Cutoff Λ_{\perp} restricts transverse momentum transfer $q_{\perp} < \Lambda_{\perp}$
(needed in eikonal limit $p \rightarrow \infty$)
- Cutoff somehow grow with jet energy
- **kinematic cutoff** $\Lambda_{\perp}^{\text{kin}}(E, T) = \zeta^{\text{kin}} g(ET)^{1/2}$
obtained from comparing leading log behavior for large p and Λ_{\perp}
- **LPM cutoff** $\Lambda_{\perp}^{\text{LPM}}(E, T) = \zeta^{\text{LPM}} g(ET^3)^{1/4}$
Estimate for momentum broadening during LPM 'formation time':
 $Q_{\perp}^2 \sim \hat{q} t^{\text{form}}, t^{\text{form}} \sim \sqrt{E/\hat{q}},$ approximately $\hat{q} \sim g^4 T^3$

[arXiv:2312.00447 [Boguslavski, Kurkela, Lappi, FL, Peuron]]

- Use cutoffs

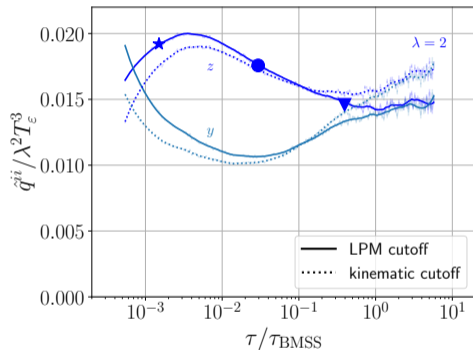
- $\Lambda_{\perp}^{\text{LPM}}(E, T_{\varepsilon}) = \zeta^{\text{LPM}} g(ET_{\varepsilon}^3)^{1/4}$

- $\Lambda_{\perp}^{\text{kin}}(E, T_{\varepsilon}) = \zeta^{\text{kin}} g(ET_{\varepsilon})^{1/2}$



[2303.12595 [Boguslavski, Kurkela, Lappi, FL, Peuron]]

- Use cutoffs
 - $\Lambda_{\perp}^{\text{LPM}}(E, T_{\varepsilon}) = \zeta^{\text{LPM}} g(ET_{\varepsilon}^3)^{1/4}$
 - $\Lambda_{\perp}^{\text{kin}}(E, T_{\varepsilon}) = \zeta^{\text{kin}} g(ET_{\varepsilon})^{1/2}$
- Fix ζ^i at triangle marker to match with JETSCAPE⁵ for $\lambda = 10$, use jet energy $E = 100$ GeV and $Q_s = 1.4$ GeV.



[2303.12595 [Boguslavski, Kurkela, Lappi, FL, Peuron]]

⁵[Phys.Rev.C 104 (2021) [JETSCAPE]]

⁶[Values available at <https://zenodo.org/records/10419537>]

Results for \hat{q}

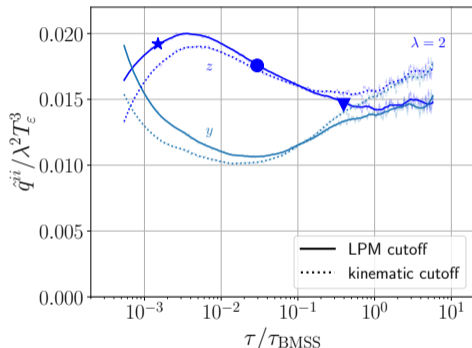
- Use cutoffs
 - $\Lambda_{\perp}^{\text{LPM}}(E, T_{\varepsilon}) = \zeta^{\text{LPM}} g(ET_{\varepsilon}^3)^{1/4}$
 - $\Lambda_{\perp}^{\text{kin}}(E, T_{\varepsilon}) = \zeta^{\text{kin}} g(ET_{\varepsilon})^{1/2}$
- Fix ζ^i at triangle marker to match with JETSCAPE⁵ for $\lambda = 10$, use jet energy $E = 100$ GeV and $Q_s = 1.4$ GeV.
- Obtain \hat{q} for multiple fixed Λ_{\perp} .

- Interpolate, using⁶

$$\hat{q}^{\text{xx}}(\Lambda_{\perp} \gg T_{\varepsilon}) \simeq a_x \ln \frac{\Lambda_{\perp}}{Q_s} + b_x$$

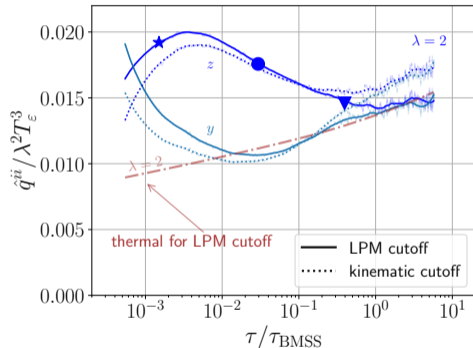
⁵[Phys.Rev.C 104 (2021) [JETSCAPE]]

⁶[Values available at <https://zenodo.org/records/10419537>]



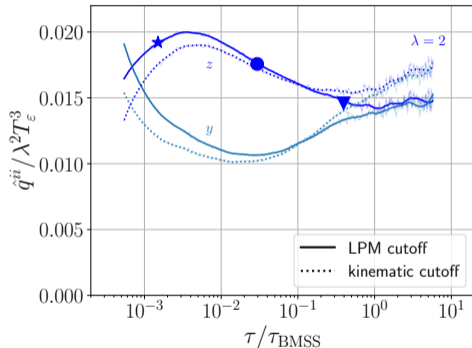
[2303.12595 [Boguslavski, Kurkela, Lappi, FL, Peuron]]

- Use cutoffs
 - $\Lambda_{\perp}^{\text{LPM}}(E, T_{\varepsilon}) = \zeta^{\text{LPM}} g(ET_{\varepsilon}^3)^{1/4}$
 - $\Lambda_{\perp}^{\text{kin}}(E, T_{\varepsilon}) = \zeta^{\text{kin}} g(ET_{\varepsilon})^{1/2}$
- Mostly $\hat{q}^{zz} > \hat{q}^{yy} \rightarrow$ **Momentum broadening along beam axis enhanced**
- Similar results for both cutoffs



[2303.12595 [Boguslavski, Kurkela, Lappi, FL, Peuron]]

- Use cutoffs
 - $\Lambda_{\perp}^{\text{LPM}}(E, T_{\varepsilon}) = \zeta^{\text{LPM}} g(ET_{\varepsilon}^3)^{1/4}$
 - $\Lambda_{\perp}^{\text{kin}}(E, T_{\varepsilon}) = \zeta^{\text{kin}} g(ET_{\varepsilon})^{1/2}$
- Mostly $\hat{q}^{zz} > \hat{q}^{yy} \rightarrow$ **Momentum broadening along beam axis enhanced**
- Similar results for both cutoffs

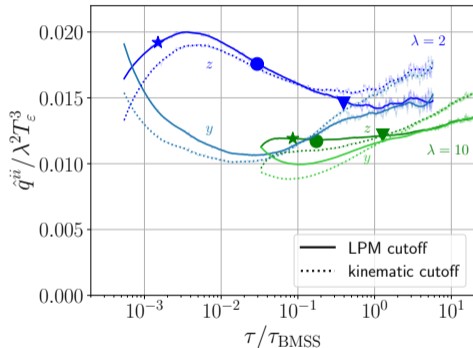


[2303.12595 [Boguslavski, Kurkela, Lappi, FL, Peuron]]

- Use cutoffs
 - $\Lambda_{\perp}^{\text{LPM}}(E, T_{\epsilon}) = \zeta^{\text{LPM}} g(ET_{\epsilon}^3)^{1/4}$
 - $\Lambda_{\perp}^{\text{kin}}(E, T_{\epsilon}) = \zeta^{\text{kin}} g(ET_{\epsilon})^{1/2}$

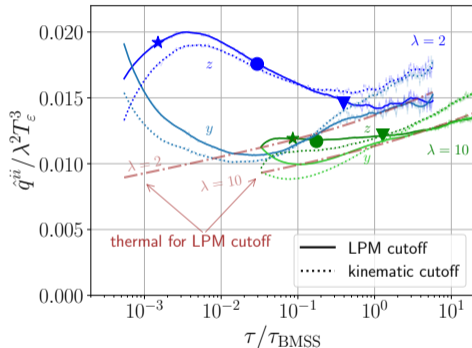
- Mostly $\hat{q}^{zz} > \hat{q}^{yy} \rightarrow$ **Momentum broadening along beam axis enhanced**

- Similar results for both cutoffs



[2303.12595 [Boguslavski, Kurkela, Lappi, FL, Peuron]]

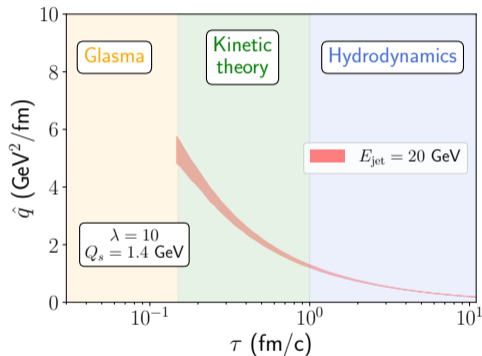
- Use cutoffs
 - $\Lambda_{\perp}^{\text{LPM}}(E, T_{\epsilon}) = \zeta^{\text{LPM}} g(ET_{\epsilon}^3)^{1/4}$
 - $\Lambda_{\perp}^{\text{kin}}(E, T_{\epsilon}) = \zeta^{\text{kin}} g(ET_{\epsilon})^{1/2}$
- Mostly $\hat{q}^{zz} > \hat{q}^{yy} \rightarrow$ **Momentum broadening along beam axis enhanced**
- Similar results for both cutoffs



[2303.12595 [Boguslavski, Kurkela, Lappi, FL, Peuron]]

Time evolution of jet quenching parameter

- Model cutoff variation for fixed jet energy
- Dependence on initial conditions and cutoff (bands)

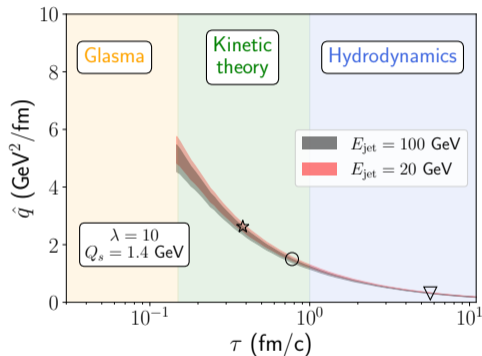


[2303.12595 [Boguslavski, Kurkela, Lappi, FL, Peuron]]

⁵[Phys.Lett.B 810 (2020) [Ipp, Müller, Schuh]]

Time evolution of jet quenching parameter

- Model cutoff variation for fixed jet energy
- Dependence on initial conditions and cutoff (bands)
- Little jet energy dependence

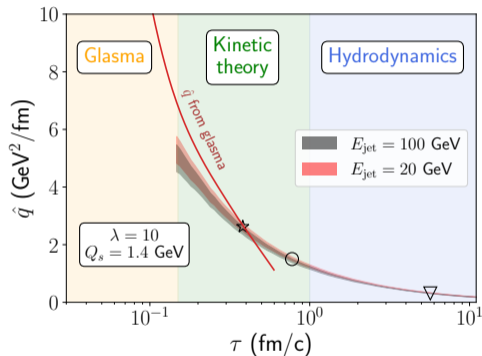


[2303.12595 [Boguslavski, Kurkela, Lappi, FL, Peuron]]

⁵[Phys.Lett.B 810 (2020) [Ipp, Müller, Schuh]]

Time evolution of jet quenching parameter

- Model cutoff variation for fixed jet energy
- Dependence on initial conditions and cutoff (bands)
- Little jet energy dependence
- Connects **large values** from **Glasma**⁵ and lower values in hydrodynamic stage

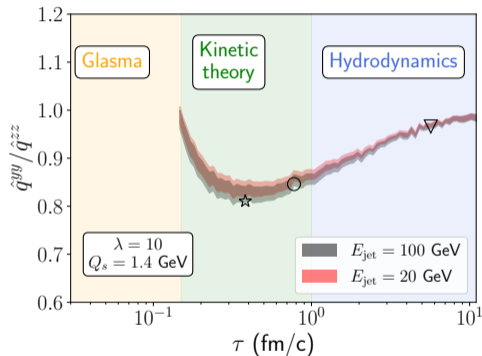


[2303.12595 [Boguslavski, Kurkela, Lappi, FL, Peuron]]

⁵[Phys.Lett.B 810 (2020) [Ipp, Müller, Schuh]]

Time evolution of jet quenching parameter

- Model cutoff variation for fixed jet energy
- Dependence on initial conditions and cutoff (bands)
- Little jet energy dependence
- Connects **large values** from **Glasma**⁵ and lower values in hydrodynamic stage

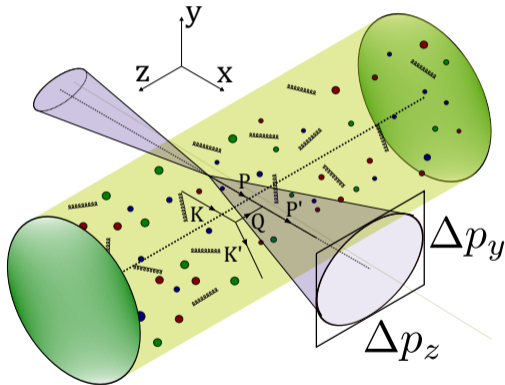


[2303.12595 [Boguslavski, Kurkela, Lappi, FL, Peuron]]

⁵[Phys.Lett.B 810 (2020) [Ipp, Müller, Schuh]]

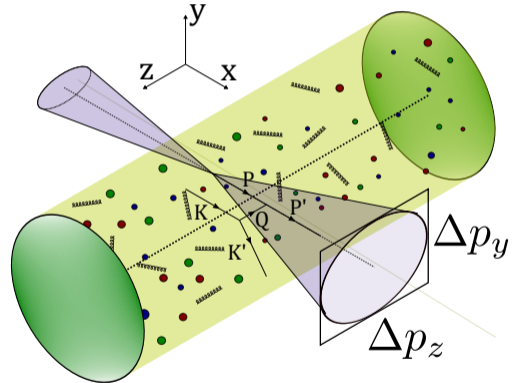
Similar in spirit: Heavy quark diffusion κ

- To study initial stages
→ very **energetic** or **heavy** probes
(must be created early)
- Here depicted: **jets**



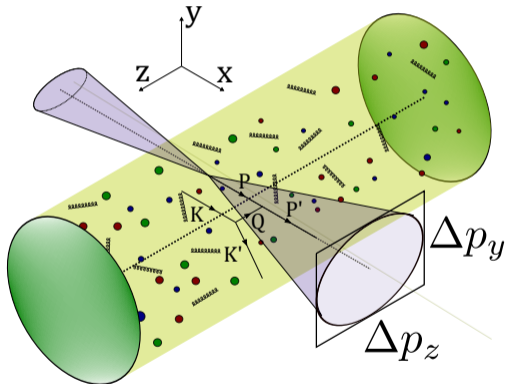
Similar in spirit: Heavy quark diffusion κ

- To study initial stages
 - very **energetic** or **heavy** probes
(must be created early)
- Here depicted: **jets**
 - **Highly energetic partons**
created in initial collision
 - Splits into many particles
→ then measured in the detectors
 - Imprints of **medium interactions**



Similar in spirit: Heavy quark diffusion κ

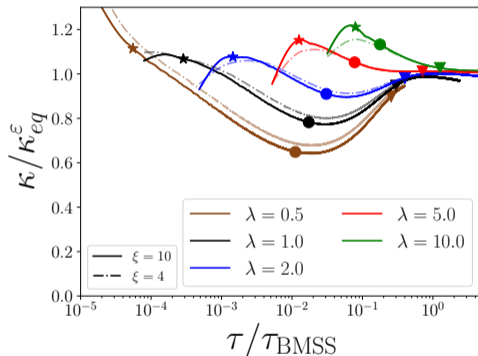
- To study initial stages
 - very **energetic** or **heavy** probes (must be created early)
- Here depicted: **jets**
 - **Highly energetic partons** created in initial collision
 - Splits into many particles → then measured in the detectors
 - Imprints of **medium interactions**
- From jets to heavy quarks:
 - **Jets:** $v \rightarrow c, m \rightarrow 0$
 - **Heavy quarks:** $v \rightarrow 0, m \rightarrow \infty$



Heavy quark diffusion coefficient κ

- Similar idea as \hat{q} : Study κ during bottom-up thermalization
- κ measures average momentum transfer to heavy quark

$$\kappa = \int d\Gamma_{\text{P}\tilde{\text{S}}} q^2 |\mathcal{M}_\kappa|^2 f(k) (1 + f(k'))$$



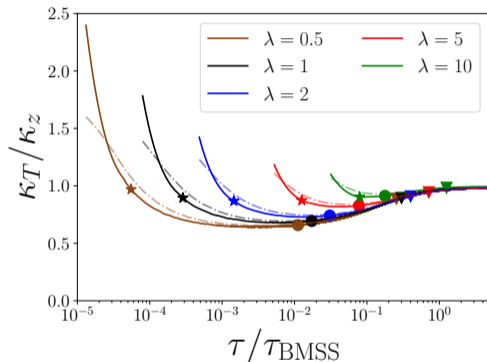
[Phys.Rev.D 109 (2024) [Boguslavski, Kärkela, Lappi, Peuron]]

Heavy quark diffusion coefficient κ

- Similar idea as \hat{q} : Study κ during bottom-up thermalization
- κ measures average momentum transfer to heavy quark

$$\kappa = \int d\Gamma_{\text{P}\ddot{\text{S}}} q^2 |\mathcal{M}_\kappa|^2 f(k) (1 + f(k'))$$

- Mostly: **more momentum transfer in beam direction**, similar to \hat{q}



[Phys.Rev.D 109 (2024) [Boguslavski, Kärkela, Läppi, FL, Peuron]]



Heavy quark diffusion coefficient κ

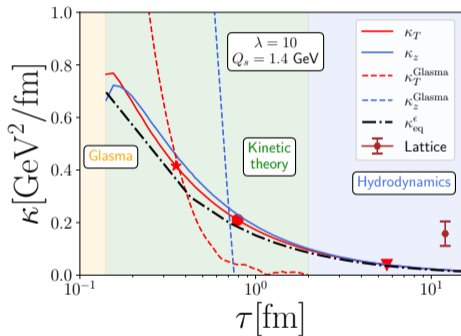
- Similar idea as \hat{q} : Study κ during bottom-up thermalization
- κ measures average momentum transfer to heavy quark

$$\kappa = \int d\Gamma_{\text{P}\ddot{\text{S}}} q^2 |\mathcal{M}_\kappa|^2 f(k) (1 + f(k'))$$

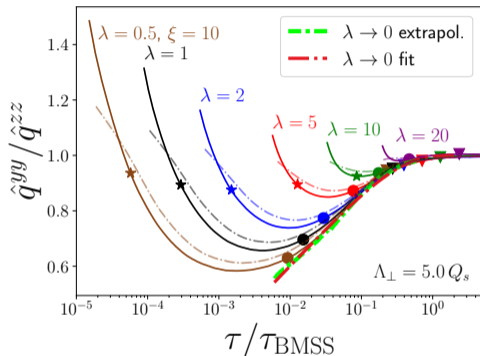
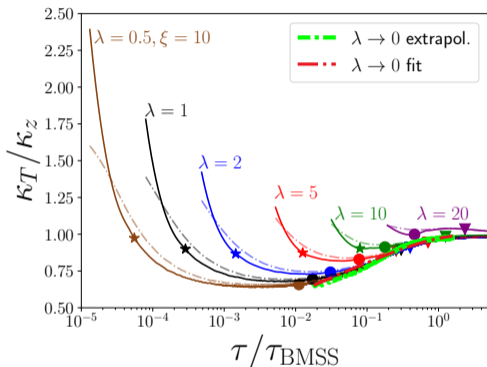
- Mostly: **more momentum transfer in beam direction**, similar to \hat{q}

[PoS HardProbes2023 (2024) [Avramescu, Bäran, Greco, Ipp, Müller, Ruggieri]]

[Phys.Rev.D 107 (2023) [Brambilla, Leino, Mayer-Staudte, Petreczky]]



[Phys.Rev.D 109 (2024) [Boguslavski, Kurkela, Lappi, FL, Peuron]]



- Approach to universal curve when scaled with $\tau_{\text{BMSS}} = \alpha^{-13/5} / Q_s$
- Many quantities plotted as function of different time ...

Conclusions and outlook

- Studied momentum broadening of jets and heavy-quarks during initial stages in heavy-ion collisions
- Values of \hat{q} and κ within 30% of thermal estimate
- \hat{q} connects to Glasma, κ shows larger deviations
- More momentum broadening along the beam axis ($\hat{q}^{zz} > \hat{q}^{yy}$)

Outlook

- Accelerating EKT simulations using machine learning
- Revisit approximations in EKT simulations (HTL-screening)
- Obtain gluon emission spectrum from pre-equilibrium \hat{q}

[Code and data: <https://zenodo.org/records/10419537>, <https://zenodo.org/records/10409474>]

Bottom-up vs. hydrodynamic attractor

- Often universal behavior in τ/τ_R ,

$$\tau_R = \frac{4\pi\eta/s}{T}.$$

Bottom-up vs. hydrodynamic attractor

- Often universal behavior in τ/τ_R ,

$$\tau_R = \frac{4\pi\eta/s}{T}.$$

- Conformal (first order) relativistic hydrodynamics ⁶:

$$\frac{P_L}{P_T} = 1 - 8 \underbrace{\frac{\eta/s}{\tau T}}_{\sim \tau_R/\tau}$$

⁶[[Romatschke, Romatschke] (2019)]

Bottom-up vs. hydrodynamic attractor

- Often universal behavior in τ/τ_R ,

$$\tau_R = \frac{4\pi\eta/s}{T}.$$

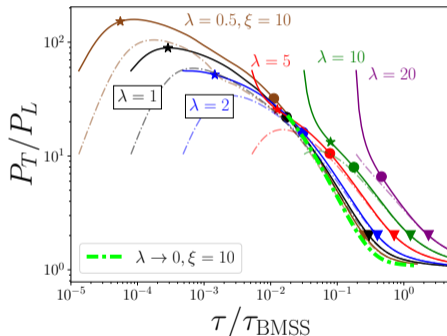
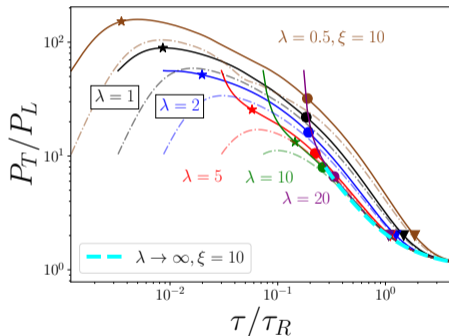
Two different pictures emerge:

- **Bottom-up** expects thermalization around $\tau_{\text{BMSS}} = \alpha_s^{-13/5}/Q_s$
- **Hydrodynamics** expects thermalization around $\tau_R = \frac{4\pi\eta/s}{T}$

How to reconcile these different time scales?

$$\tau_R = \frac{4\pi\eta/s}{T}, \quad \tau_{\text{BMSS}} = \alpha_s^{-13/5} / Q_s$$

- Kinetic theory simulations for different couplings $0.5 \leq \lambda \leq 20$ and initial conditions.

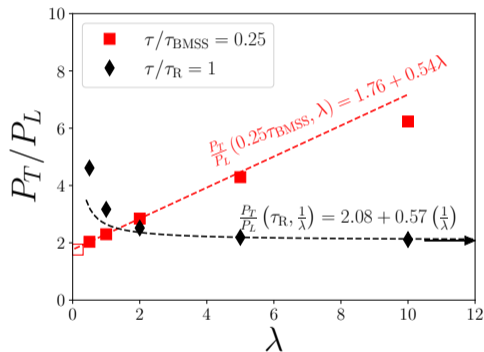


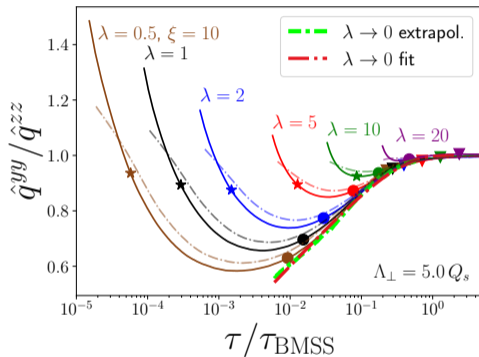
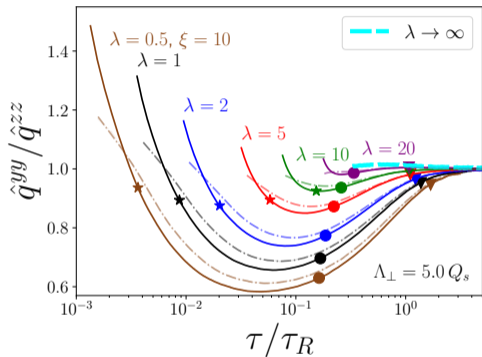
- Attractor for each λ (insensitive to IC)
- Curves approach limiting attractors after •

$$\tau_R = \frac{4\pi\eta/s}{T}$$

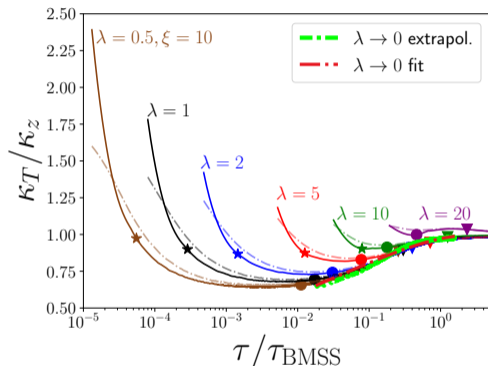
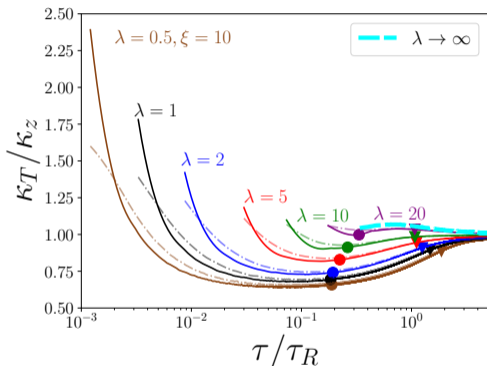
$$\tau_{\text{BMSS}} = \alpha_s^{-13/5} / Q_s$$

- Obtain limiting attractors by extrapolating at fixed τ/τ_R or τ/τ_{BMSS}
- **Bottom-up attractor**: Linear extrapolation to $\lambda \rightarrow 0$
- **Hydro attractor**: Linear extrapolation to $1/\lambda \rightarrow 0$





- Approach to weak coupling attractor even at moderate couplings



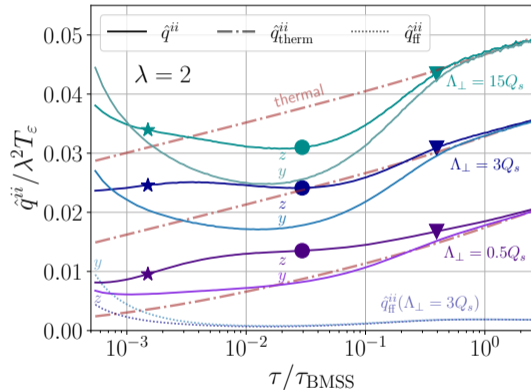
- Similar to \hat{q} : Approach to weak coupling attractor even at moderate λ

- \hat{q} for fixed coupling $\lambda = 2$ and varying cutoffs Λ_{\perp}
- 2D distribution

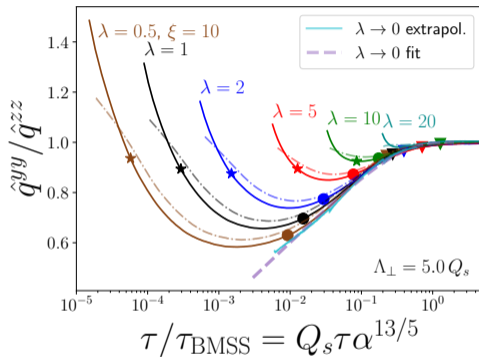
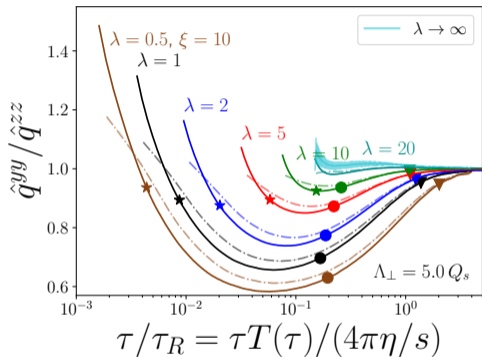
$$f(\mathbf{k}) \sim \delta(k_z)$$

Leads to $\hat{q}_{\text{ff}}^{zz} = 0$

- Reason for different ordering: Bose-enhanced part \hat{q}_{ff} = term quadratic in $f(\mathbf{k})$



\hat{q} and the limiting attractors



- Approach to weak coupling attractor even at moderate couplings

- Fit for bottom-up attractor:

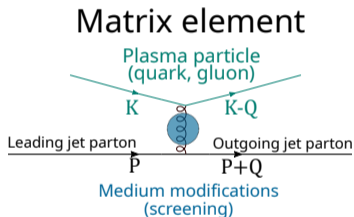
$$\frac{\hat{q}^{yy}}{\hat{q}^{zz}}(\tau) \approx 1 + c_1 \ln(1 - e^{-c_2 \tau / \tau_{\text{BMSS}}}) \text{ with } c_1 = 0.12, c_2 = 3.45.$$

Screening in the matrix element of \hat{q}

- Scattering matrix element includes **in-medium propagator**
 - Receives **self-energy corrections**
 - Anisotropic hard thermal loop (HTL) self-energy \rightarrow unstable modes⁶
 - **Approximation: Use isotropic HTL matrix element**
- Similar approximation also in EKT implementations⁷

⁶[Phys.Rev.D 68 (2003) [Romatschke, Strickland]]

⁷[Phys.Rev.Lett. 115 (2015) [Kurkela, Zhu]; Phys.Rev.Lett. 122 (2019) [Kurkela, Mazeliauskas]; Phys.Rev.D 104 (2021) [Du, Schlichting]]

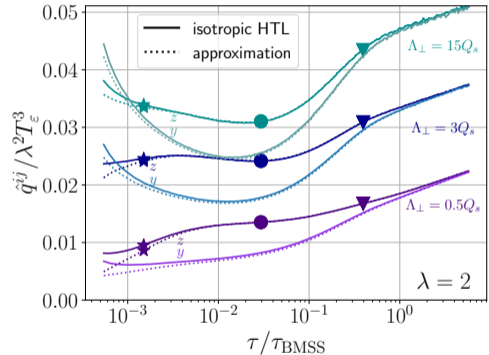


Screening approximation to the matrix element

- Compare with simple screening approximation

$$\frac{(s-u)^2}{t^2} \rightarrow \frac{(s-u)^2}{t^2} \frac{q^4}{(q^2 + \xi_T^2 m_D^2)^2}$$

- Longitudinal⁸ $\xi_L = e^{5/6}/\sqrt{8}$
- Transverse broadening:
 $\xi_T = e^{1/3}/2$
- **Good agreement**

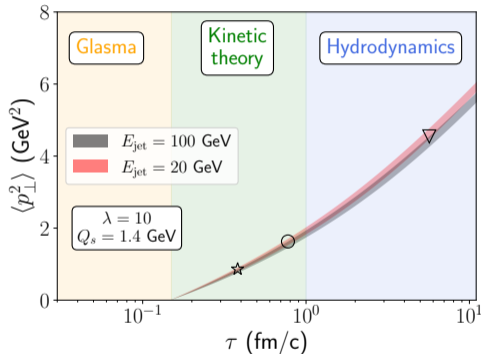


s, u, t : Mandelstam variables

⁸[Phys.Rev.D 89 (2014) [York, Kurkela, Lu, Moore]]

What about momentum broadening?

- Per definition, $\hat{q} = \frac{d\langle p_{\perp}^2 \rangle}{d\tau}$
- Naively $\Delta p_{\perp}^2 = \int d\tau \hat{q}(\tau)$ over lifetime of jet
- But: only true if no splittings occur.
- Think of \hat{q} as medium parameter.



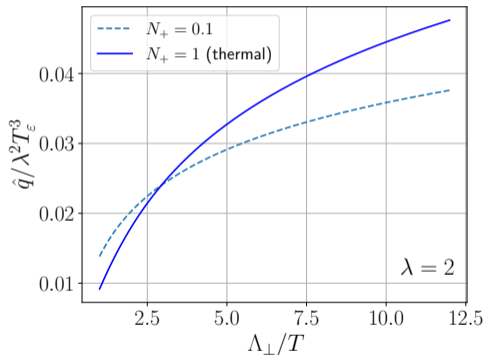
- Scaled thermal distribution

$$f(k; T) = \frac{N_+}{\exp(k/T) - 1}$$

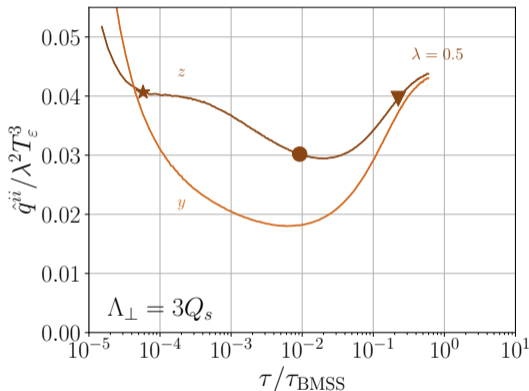
Explains ordering $\hat{q}_{\text{therm}} \lesssim \hat{q}$ for underoccupancy

[arXiv:2312.00447 [Boguslavski, Kurkela, Lappi, FL, Peuron]]

Scaled thermal distribution

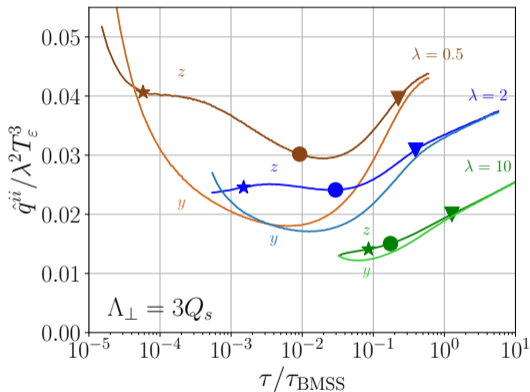


- Landau matching
 $\varepsilon^{\text{eq}}(T_\varepsilon) = \varepsilon^{\text{sim}}$
- Obtain \hat{q}^{ii} for a fixed cutoff Λ_\perp
- For coupling $\lambda = 0.5$
- Mostly $\hat{q}^{zz} > \hat{q}^{yy} \rightarrow$
**Momentum broadening
 along beam axis enhanced**

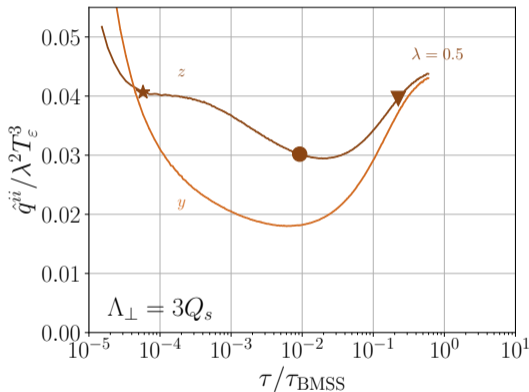


Time evolution of \hat{q}

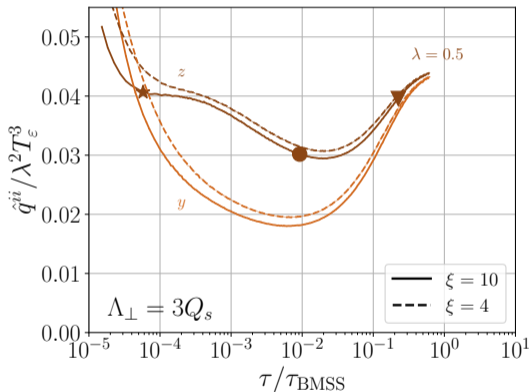
- Landau matching
 $\varepsilon^{\text{eq}}(T_\varepsilon) = \varepsilon^{\text{sim}}$
- Obtain \hat{q}^{ii} for a fixed cutoff Λ_\perp
- For couplings $\lambda = 0.5, 2, 10$
- Mostly $\hat{q}^{zz} > \hat{q}^{yy} \rightarrow$
**Momentum broadening
along beam axis enhanced**



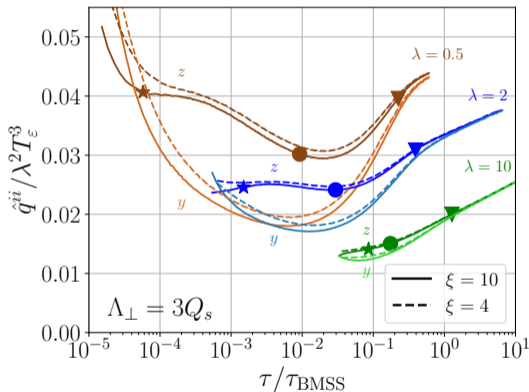
- Landau matching
 $\varepsilon^{\text{eq}}(T_\varepsilon) = \varepsilon^{\text{sim}}$
- Obtain \hat{q}^{ii} for a fixed cutoff Λ_\perp
- For coupling $\lambda = 0.5$
- Mostly $\hat{q}^{zz} > \hat{q}^{yy} \rightarrow$
**Momentum broadening
along beam axis enhanced**



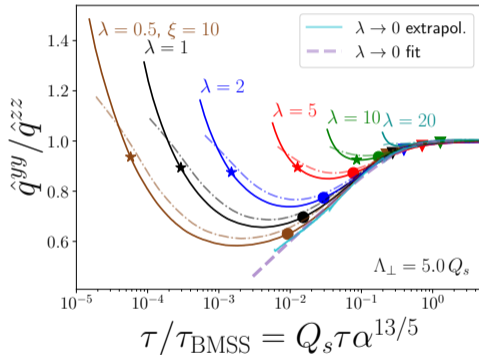
- Landau matching
 $\varepsilon^{\text{eq}}(T_\varepsilon) = \varepsilon^{\text{sim}}$
- Obtain \hat{q}^{ii} for a fixed cutoff Λ_\perp
- For coupling $\lambda = 0.5$
- Mostly $\hat{q}^{zz} > \hat{q}^{yy} \rightarrow$
**Momentum broadening
along beam axis enhanced**
- Weak dependence on initial
anisotropy ξ



- Landau matching
 $\varepsilon^{\text{eq}}(T_\varepsilon) = \varepsilon^{\text{sim}}$
- Obtain \hat{q}^{ii} for a fixed cutoff Λ_\perp
- For couplings $\lambda = 0.5, 2, 10$
- Mostly $\hat{q}^{zz} > \hat{q}^{yy} \rightarrow$
**Momentum broadening
along beam axis enhanced**
- Weak dependence on initial anisotropy ξ

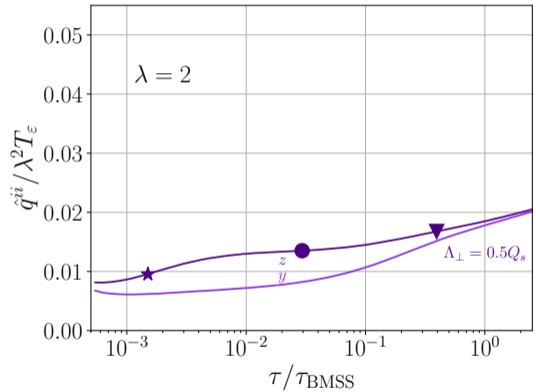


- Ratio $\hat{q}^{yy} / \hat{q}^{zz}$ follows attractor in thermalization time τ_{BMSS}
 \rightarrow “bottom-up limiting attractor”⁹



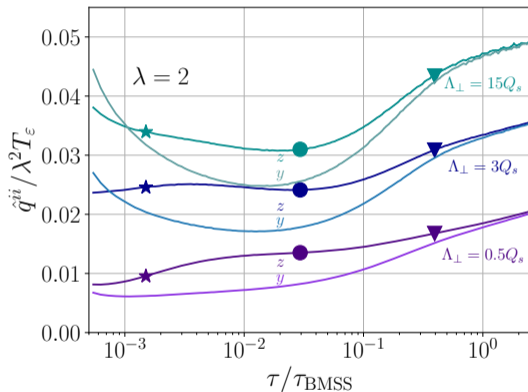
⁹[arXiv:2312.11252 [Boguslavski, Kurkela, Lappi, FL, Peuron]]

- \hat{q} for fixed coupling $\lambda = 2$



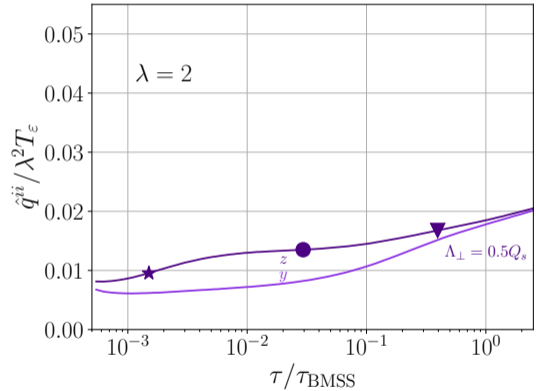
Cutoff dependence and comparison with equilibrium

- \hat{q} for fixed coupling $\lambda = 2$ and varying cutoffs Λ_{\perp}
- Ordering $\hat{q}^{yy} \lesseqgtr \hat{q}^{zz}$ depends on cutoff



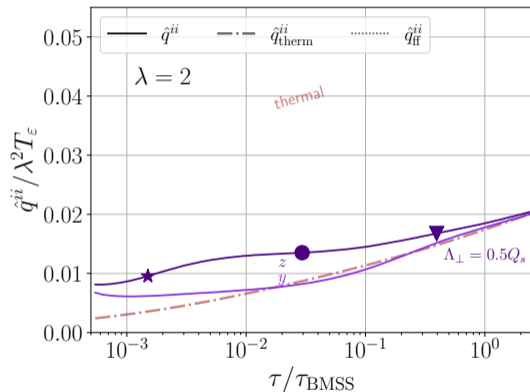
Cutoff dependence and comparison with equilibrium

- \hat{q} for fixed coupling $\lambda = 2$ and varying cutoffs Λ_{\perp}
- **Ordering $\hat{q}^{yy} \lesseqgtr \hat{q}^{zz}$ depends on cutoff**



Cutoff dependence and comparison with equilibrium

- \hat{q} for fixed coupling $\lambda = 2$ and varying cutoffs Λ_{\perp}
- **Ordering** $\hat{q}^{yy} \lesseqgtr \hat{q}^{zz}$ **depends on cutoff**
- Compare with **energy-density matched thermal equilibrium**



Cutoff dependence and comparison with equilibrium

- \hat{q} for fixed coupling $\lambda = 2$ and varying cutoffs Λ_{\perp}
- Ordering $\hat{q}^{yy} \leq \hat{q}^{zz}$ depends on cutoff
- Energy-matched equilibrium over- or underestimates \hat{q} , depending on cutoff

